PHYSICAL REVIEW C **87**, 021303(R) (2013)

Ab initio calculations of medium-mass nuclei with explicit chiral 3*N* interactions

Sven Binder,[1,*] Joachim Langhammer,[1] Angelo Calci,[1] Petr Navrátil,[2] and Robert Roth[1]
[1]*Institut für Kernphysik, Technische Universität Darmstadt, 64289 Darmstadt, Germany*
[2]*TRIUMF, 4004 Wesbrook Mall, Vancouver, British Columbia V6T 2A3, Canada*
(Received 20 November 2012; published 21 February 2013)

We present the first *ab initio* coupled-cluster calculations of medium-mass nuclei with explicit chiral three-nucleon (3*N*) interactions. Using a spherical formulation of coupled cluster with singles and doubles excitations including explicit 3*N* contributions, we study ground states of ^{16,24}O, ^{40,48}Ca, and ^{56}Ni. We employ chiral nucleon-nucleon (*NN*) plus 3*N* interactions softened through a similarity renormalization group (SRG) transformation at the three-body level. We investigate the impact of all truncations and quantify the resulting uncertainties—this includes the contributions from triple excitations, the truncation of the set of three-body matrix elements, and the omission of SRG-induced four-body interactions. Furthermore, we assess the quality of a normal-ordering approximation of the 3*N* interaction beyond light nuclei. Our study points towards the predictive power of chiral Hamiltonians in the medium-mass regime.

DOI: 10.1103/PhysRevC.87.021303 PACS number(s): 21.30.−x, 05.10.Cc, 21.45.Ff, 21.60.De

The *ab initio* description of medium-mass nuclei is one of the most dynamic frontiers in nuclear structure theory today—bridging the gap between accurate *ab initio* calculations for light nuclei and the realm of approximate or phenomenological approaches for heavy nuclei and nuclear matter. A number of many-body methods are being developed and extended towards the medium-mass regime. Coupled-cluster (CC) theory has a pioneering role in this domain [1–3] and other methods, like self-consistent Green's function approaches [4] or the in-medium similarity renormalization group [5,6], have followed. Extensions of the no-core shell model (NCSM) [7], like the importance-truncated NCSM [8,9], are connecting the domains of light- and medium-mass nuclei.

A critical ingredient for all *ab initio* many-body approaches is the Hamiltonian. At present, chiral effective field theory (EFT) provides the most systematic approach to QCD-based Hamiltonians for accurate nuclear structure calculations [10,11]. Already the present generation of chiral Hamiltonians, consisting of nucleon-nucleon (*NN*) interactions at next-to-next-to-next-to-leading order (N^{3}LO) [12,13] and three-nucleon (3*N*) interactions at next-to-next-to-leading order (N^{2}LO) [14], gives a very good description of *p*-shell nuclei as demonstrated in *ab initio* NCSM calculations [15–18]. Ongoing developments in this sector, e.g., regarding chiral 3*N* interactions at N^{3}LO [19–21] or a Δ-full formulation of chiral EFT [22], will soon provide next-generation chiral Hamiltonians with consistent *NN* and 3*N* interactions.

The inclusion of the 3*N* interaction is vital to realize the predictive potential of chiral Hamiltonians but poses a number of computational challenges. So far, there are no calculations for medium-mass nuclei that include explicit chiral 3*N* interactions, without resorting to approximate or even schematic reductions to effective two-body interactions [3,23]. A systematic though approximate inclusion of chiral 3*N* interactions for medium-mass nuclei is the normal-ordering scheme applied in Ref. [24].

In this Rapid Communication we present *ab initio* coupled-cluster calculations for medium-mass nuclei including explicit 3*N* interactions. We have developed a spherical implementation of coupled cluster with single and double excitations for three-body Hamiltonians (CCSD3B), which enables us to perform converged ground-state calculations for closed-shell nuclei with full three-body interactions. In this framework we study the ground-state energies of ^{16,24}O, ^{40,48}Ca, and ^{56}Ni using chiral $NN + 3N$ Hamiltonians softened through similarity renormalization group (SRG) transformations [18,25]. We systematically address all truncations introduced in the many-body framework and the Hamiltonian and quantify the resulting uncertainties in the ground-state energies. We demonstrate that the overall uncertainty for the prediction of ground-state energies in the medium-mass regime is of the order of a few percent. Within these uncertainties the chiral $NN + 3N$ Hamiltonians used in this work predict ground-state energies that are in agreement with experiments. This is a remarkable result, since no information beyond the few-body domain ($A \leqslant 4$) was used to fix the parameters of the chiral interactions.

Coupled-cluster method. In single-reference CCSD the ground state $|\Psi\rangle$ of a many-body Hamiltonian is parametrized by the exponential ansatz

$$|\Psi\rangle = e^T |\Phi\rangle \tag{1}$$

with $T = T_1 + T_2$, where T_n are excitation operators of the form

$$T_n = \frac{1}{(n!)^2} \sum_{\substack{a_1 \ldots a_n \\ i_1 \ldots i_n}} \langle a_1 \ldots a_n | t_n | i_1 \ldots i_n \rangle \, a^\dagger_{a_1} \ldots a^\dagger_{a_n} a_{i_n} \ldots a_{i_1}, \tag{2}$$

acting on a single Slater-determinant reference state $|\Phi\rangle$.

Coupled-cluster theory is conveniently formulated in terms of Hamiltonians that are normal ordered with respect to $|\Phi\rangle$. If the original Hamiltonian

$$H = h_1 + h_2 + h_3 \tag{3}$$

*sven.binder@physik.tu-darmstadt.de

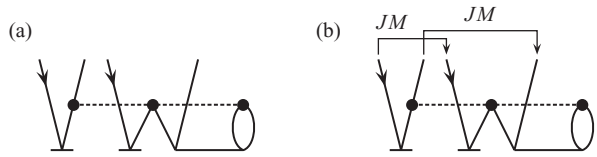

FIG. 1. One example diagram contributing to the CCSD3B T_2 amplitude equations in the m scheme (a) and the spherical scheme (b).

consisting of one-, two-, and three-body contributions is cast into normal-ordered form,

$$H = \langle\Phi|H|\Phi\rangle + h_1^{\rm NO} + h_2^{\rm NO} + h_3^{\rm NO}, \tag{4}$$

contributions from the n-body part h_n of the original Hamiltonian enter the matrix elements of the normal-ordered operators $h_k^{\rm NO}$ of particle ranks $k \leqslant n$.

Neglecting the three-body part $h_3^{\rm NO}$ of the normal-ordered Hamiltonian (4) and thus only including contributions of the three-body interaction that have been demoted to lower particle ranks through normal-ordering leads to the normal-ordering approximation (NO2B) discussed in Refs. [24,26]. In this Rapid Communication we include the complete $3N$ interaction; i.e., we include the normal-ordered three-body part $h_3^{\rm NO}$ beyond the NO2B approximation explicitly. The CCSD energy and amplitude equations including the full $3N$ interaction can be written as

$$\Delta E = \Delta E_{\rm NO2B} + \langle\Phi|\, h_3^{\rm NO}\, e^T\, |\Phi\rangle_C, \tag{5}$$

$$0 = T_{1,\rm NO2B} + \left\langle\Phi_i^a\right|\, h_3^{\rm NO}\, e^T\, |\Phi\rangle_C, \tag{6}$$

$$0 = T_{2,\rm NO2B} + \left\langle\Phi_{ij}^{ab}\right|\, h_3^{\rm NO}\, e^T\, |\Phi\rangle_C, \tag{7}$$

where $\Delta E_{\rm NO2B}$ and $T_{n,\rm NO2B}$ denote the standard CCSD equations for two-body Hamiltonians [27] corresponding to the NO2B approximation. Thus, the inclusion of the residual three-body operator $h_3^{\rm NO}$ generates a set of additional terms in the CCSD equations.

Expressions for Eqs. (5)–(7) in the m scheme are presented in a factorized form in Ref. [26]. We rederived these equations in a straightforward unfactorized way, resulting in more but simpler terms. Already for two-body Hamiltonians the basis sizes and particle numbers for m-scheme CC calculations are severely limited by the number of amplitudes and matrix elements that need to be handled. It is well known that the range of the CC method can be greatly extended by exploiting spherical symmetry and using an angular-momentum coupled formulation [28]. We have developed such an efficient spherical implementation of CCSD3B. Proceeding along the lines of Ref. [28], we couple the external lines of the diagrams, cut open internal lines and perform angular momentum recouplings in order to express diagrams in terms of angular-momentum coupled matrix elements of the operators involved. For example, one of the computationally more involved contributions [Fig. 1(a)] to the T_2 amplitude equations reads in m scheme as

$$\frac{1}{4}\, P_{ab}\, P_{ij} \sum_{cdekl} \langle kla|h_3^{\rm NO}|cde\rangle\, \langle eb|t_2|kl\rangle\, \langle c|t_1|i\rangle\, \langle d|t_1|j\rangle, \tag{8}$$

where we use the standard diagrammatic representation [27] and the permutation operator $P_{pq} = 1 - T_{pq}$ with T_{pq} denoting index transpositions. The corresponding contribution [Fig. 1(b)] in the spherical scheme is given by

$$-\frac{1}{4}\, P_{ab}^{(J)}\, P_{ij}^{(J)}\, \left(\hat{J}\hat{j}_i\hat{j}_j\right)^{-1}\, (-1)^{j_a+j_b-J} \sum_{cdekl} \sum_{J'J''} \hat{J}'\,\hat{J}''$$
$$\times \begin{Bmatrix} J' & J'' & J \\ j_a & j_b & j_e \end{Bmatrix} \langle kl\tilde{a}||h_3^{\rm NO}||\tilde{cde}\rangle\, \langle eb|t_2|kl\rangle\, \langle\tilde{c}|t_1|i\rangle\, \langle\tilde{d}|t_1|j\rangle \tag{9}$$

with $P_{pq}^{(J)} = 1 - (-1)^{j_p+j_q-J} T_{pq}$ and $\hat{x} = \sqrt{2x+1}$. Here, indices $a, b, \ldots$ represent (nlj) orbitals rather than individual single-particle states. The coupling lines indicate standard angular-momentum coupling and the tilde denotes time-reversed orbitals.

In our spherical scheme, the three-body matrix elements of $h_3^{\rm NO}$ enter in a specific reduced and coupled form, given by

$$\langle\tilde{abc}||h_3^{\rm NO}||\tilde{def}\rangle = \sum_J (-1)^{J-j_c-J_{ab}}\, \hat{J}_{cf}\hat{J}^2 \begin{Bmatrix} J_{ab} & J_{de} & J_{cf} \\ j_f & j_c & J \end{Bmatrix}$$
$$\times \langle[(ab)J_{ab}c]JM|h_3^{\rm NO}|[(de)J_{de}f]JM\rangle \tag{10}$$

where the $3N$ matrix element on the right-hand side is M independent. We use this specific coupling to store the three-body matrix elements in fast memory, making use of a variant of the efficient storage and retrieval schemes we have developed for JT-coupled three-body matrix elements [18,29]. This is critical for the overall performance of the CCSD3B calculations. In order to accelerate the convergence of the iterative solution of the CCSD3B amplitude equations, we initialize the amplitudes with the solution of the corresponding CCSD calculation in the NO2B approximation. In addition to the CCSD and CCSD3B calculations we perform Λ-CCSD(T) calculations [28,30,31] using the NO2B Hamiltonian to assess the influence of triple excitations.

Hamiltonian and basis. The starting point for our investigation of medium-mass nuclei is SRG-evolved chiral $NN + 3N$ Hamiltonians. We use the chiral NN interaction at N^{3}LO [12] and a local form of the chiral $3N$ interaction at N^{2}LO [14]. Instead of a momentum cutoff of 500 MeV used, e.g., in Ref. [18], we reduce the cutoff of the initial $3N$ interaction to 400 MeV and choose $c_E = 0.098$ to reproduce the ^{4}He ground-state energy, keeping $c_D = -0.2$ [24]. This cutoff reduction is motivated by the observation that SRG-induced $4N$ interactions have a sizable impact on ground-state energies of medium-mass nuclei, which can be reduced efficiently by reducing the cutoff of the initial $3N$ interaction [18,24,29]. We emphasize that the following results for medium-mass nuclei from ^{16}O to ^{56}Ni are pure predictions.

We employ two types of SRG-evolved Hamiltonians: The $NN + 3N$–full Hamiltonian starts with the initial chiral $NN + 3N$ Hamiltonian and retains all terms up to the $3N$ level in the SRG evolution, the $NN + 3N$–induced Hamiltonian omits the chiral $3N$ interaction from the initial Hamiltonian

but keeps all induced $3N$ terms throughout the evolution. In addition, we use a range of flow parameters α in order to assess the role of SRG-induced contributions beyond the three-body level [18].

The underlying single-particle basis is a harmonic-oscillator basis truncated in the principal oscillator quantum number $2n + l = e \leqslant e_{\max}$ and we go up to $e_{\max} = 12$. We perform Hartree-Fock (HF) calculations including the $3N$ interaction for each set of basis parameters to obtain an optimized single-particle basis and stabilize the convergence of the CC iterations. The normal-ordering is done consistently, i.e., with respect to the HF reference state. At the moment it is not possible to include all three-body matrix elements that would appear in the larger bases; we are limited to three-body matrix elements with $e_1 + e_2 + e_3 \leqslant E_{3\max} = 14$. We discuss the impact of this additional cut in detail later on. We stress that the exact treatment of the isospin dependence of the two- and three-body matrix elements in the HF basis is crucial. It is generated by isospin dependence of the HF single-particle wave functions, although the $3N$ operator used here is isospin symmetric. In order to avoid a drastic increase of storage needed for the HF three-body matrix elements, we perform the transformation to the HF basis on the fly.

Results. We present first results of CC calculations with explicit $3N$ interactions for the ground-state energies of ^{16,24}O, ^{40,48}Ca, and ^{56}Ni. Step by step, we quantify the uncertainties resulting from various truncations in the many-body treatment. First we contrast CCSD3B calculations with CCSD using the NO2B approximation for the Hamiltonian. For both we discuss basis-space convergence in terms of $e_{\max}$ and oscillator frequency $\hbar\Omega$. We then study the influence of the three-body truncation $E_{3\max}$. Finally, we include noniterative triples corrections at the level of Λ-CCSD(T) with the NO2B Hamiltonian. In all cases we vary the flow parameter α over a wide range to study the impact of induced many-body terms.

Figure 2 shows a comparison of CCSD3B calculations using the complete $3N$ interaction with CCSD using the NO2B approximation for the ground-state energies of ^{16,24}O, ^{40,48}Ca, and ^{56}Ni as function of the basis size $e_{\max}$ for both the $NN + 3N$–induced and the $NN + 3N$–full Hamiltonian with three different values of the SRG flow parameter. The oscillator frequencies correspond to the energy minima in the largest basis spaces (cf. Fig. 3). The numerical values of the ground-state energies for the largest basis sets are also summarized in Tables I and II. The first observation is that we are able to converge or come sufficiently close to convergence with respect to the basis size $e_{\max}$ in practically all cases. The second observation is that the NO2B works extremely well for all cases: For ^{16}O the largest deviation from the full CCSD3B results is 0.9 MeV or 0.8%, for ^{56}Ni it is 4 MeV or 0.8% across all Hamiltonians considered here. Given that the computational cost for the CCSD3B calculations is two orders of magnitude higher than for CCSD and that the accuracy we target for many-body calculations in this mass range is not better than 1%, the NO2B approximation constitutes a very efficient tool.

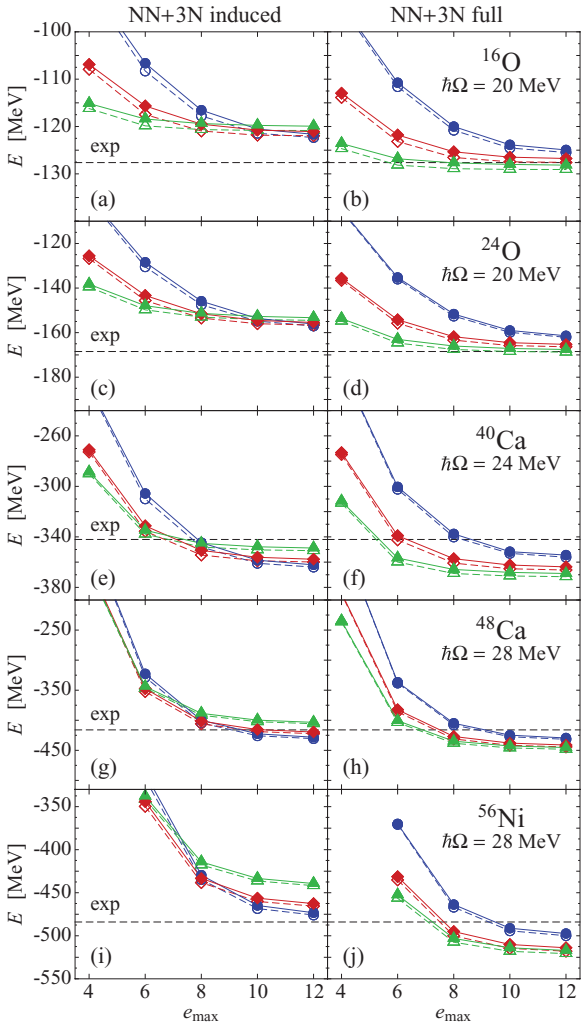

FIG. 2. (Color online) Ground-state energies for ^{16,24}O, ^{40,48}Ca, and ^{56}Ni as function of $e_{\max}$ for the two types of Hamiltonians (see column headings) using CCSD3B (solid lines) and the NO2B approximation (dashed lines) for a range of flow parameters: $\alpha =$ 0.02 fm^4 (●), 0.04 fm^4 (◆), 0.08 fm^4 (▲).

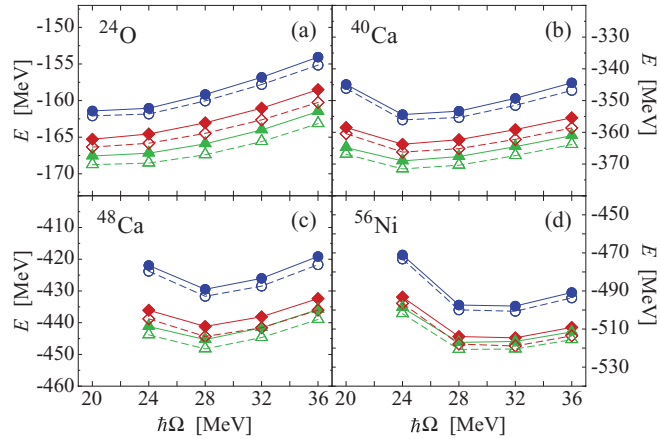

FIG. 3. (Color online) Ground-state energies for ^{24}O, ^{40,48}Ca, and ^{56}Ni as function of $\hbar\Omega$ at $e_{\max} = 12$ for the $NN + 3N$–full Hamiltonian using CCSD3B (solid lines) and the NO2B approximation (dashed lines) for a range of flow parameters: $\alpha = 0.02$ fm^4 (●), 0.04 fm^4 (◆), and 0.08 fm^4 (▲).

TABLE I. Summary of CCSD and Λ-CCSD(T) ground-state energies in MeV for the $NN + 3N$–induced Hamiltonian for a subset of α values computed at optimum oscillator frequency $\hbar\Omega = 20$ MeV for ^{16,24}O, $\hbar\Omega = 24$ MeV for ^{40}Ca, and $\hbar\Omega = 28$ MeV for ^{48}Ca, ^{56}Ni. The number in parentheses denotes the $E_{3\,\mathrm{max}}$ cut in the $3N$ Hamiltonian. The last column gives e_{max}-extrapolated values, and the other columns are for $e_{\mathrm{max}} = 12$.

$NN + 3N$	α (fm^4)	CCSD	CCSD		Λ-CCSD(T)	
induced		3B (12)	NO2B (12)	NO2B (14)	NO2B (14)	NO2B$^\infty$ (14)
^{16}O	0.02	−121.6	−122.3	−121.7	−126.1	−126.5
	0.04	−121.1	−121.9	−121.6	−124.4	−124.4
	0.08	−119.9	−120.8	−120.8	−122.4	−122.4
^{24}O	0.02	−156.1	−157.0	−155.8	−162.7	−163.7
	0.04	−155.4	−156.6	−155.9	−160.2	−160.4
	0.08	−153.3	−154.5	−154.4	−156.9	−157.1
^{40}Ca	0.02	−362.1	−363.9	−360.5	−374.3	−375.5
	0.04	−357.7	−359.9	−358.1	−366.3	−366.6
	0.08	−348.8	−350.9	−350.8	−355.3	−355.5
^{48}Ca	0.02	−428.1	−430.5	−425.3	−442.3	−443.9
	0.04	−419.6	−422.3	−420.0	−429.6	−430.9
	0.08	−403.4	−405.7	−406.8	−411.9	−413.3
^{56}Ni	0.02	−473.2	−475.8	−464.3	−487.5	−489.8
	0.04	−462.6	−465.6	−458.0	−472.4	−474.2
	0.08	−439.3	−441.8	−439.3	−448.4	−450.4

The quality of the NO2B approximation is confirmed in Fig. 3, where it is compared to CCSD3B using the $NN + 3N$–full Hamiltonian and the largest basis set as function of the oscillator frequency. The accuracy of the NO2B approximation is largely independent of $\hbar\Omega$. Note that the effect of the residual $3N$ interaction beyond the NO2B approximation is always repulsive, i.e., of the same sign as the complete $3N$ contribution composed of induced and evolved initial $3N$ terms [24].

The fact that the SRG evolution in the $3N$ sector is performed in a finite model space of harmonic-oscillator Jacobi states [18,29] leads to additional uncertainties at low frequencies $\hbar\Omega$. By varying the size of SRG model space [29] we estimate the uncertainties at the optimal frequency to be much smaller than 1% for all nuclei except ^{56}Ni, where they reach the 1% level. For smaller frequencies, however, the truncation of the SRG model space leads to more significant effects—the increase of the ground-state energies of ^{40}Ca and beyond at the lowest frequencies shown in Fig. 3 as well as the shift of the optimal frequency to larger values for heavier nuclei are partly due to this.

Next we address the $E_{3\,\mathrm{max}}$ cut used in the $3N$ matrix elements for technical reasons. In Tables I and II the CCSD

TABLE II. Same as in Tab. I for the $NN + 3N$-full Hamiltonian.

$NN + 3N$	α (fm^4)	CCSD	CCSD		Λ-CCSD(T)	
full		3B (12)	NO2B (12)	NO2B (14)	NO2B (14)	NO2B$^\infty$ (14)
^{16}O	0.02	−124.9	−125.4	−124.5	−129.9	−130.4
	0.04	−126.8	−127.6	−127.1	−130.8	−130.8
	0.08	−128.2	−129.1	−129.0	−131.2	−131.2
^{24}O	0.02	−161.4	−162.0	−160.4	−168.3	−169.4
	0.04	−165.3	−166.4	−165.5	−170.7	−170.9
	0.08	−167.6	−168.8	−168.6	−171.6	−171.7
^{40}Ca	0.02	−354.4	−356.0	−352.1	−370.6	−371.7
	0.04	−363.8	−366.2	−364.3	−376.4	−376.7
	0.08	−369.0	−371.5	−371.3	−378.2	−378.4
^{48}Ca	0.02	−429.4	−431.6	−426.7	−449.5	−450.9
	0.04	−441.2	−444.3	−441.9	−456.0	−457.0
	0.08	−445.3	−448.2	−448.3	−453.5	−456.7
^{56}Ni	0.02	−497.3	−499.9	−490.9	−521.7	−523.4
	0.04	−513.9	−517.9	−511.4	−530.9	−531.8
	0.08	−517.0	−520.7	−517.9	−528.4	−529.2

results using the NO2B approximation with $E_{3\,\max} = 12$ and 14 are compared. We find that the influence of this cut grows with increasing particle number and decreasing flow parameter α. For the softest interaction with $\alpha = 0.08\,\mathrm{fm}^4$ the cut is completely irrelevant up to ^{40}Ca; only for ^{56}Ni we observe a 0.5% change in the ground-state energy. For less evolved interactions the effect increases and reaches about 1% up to ^{48}Ca and about 2% for ^{56}Ni. For the description of still heavier nuclei or the use of bare $3N$ interactions one will have to improve on this truncation in order to reach accurate results.

As the final model-space-related truncation, we discuss the truncation of the excitation operators in the coupled-cluster ansatz (1). In Fig. 4 we compare the results of CCSD and Λ-CCSD(T) calculations for all nuclei and Hamiltonians in the NO2B approximation as function of the basis truncation $e_{\max}$ for $E_{3\,\max} = 14$. The results for $e_{\max} = 12$ are also summarized in Tables I and II. Again we observe a systematic dependence on the flow parameter α. For the softest interactions with $\alpha = 0.08\,\mathrm{fm}^4$ the inclusion of triple excitations lowers the ground-state energies by 1.5 to 2% for all nuclei and both Hamiltonians. For $\alpha = 0.02\,\mathrm{fm}^4$ the difference increases to about 4 to 6%. If we conservatively consider the triple contribution as a measure for the inherent uncertainty due to the truncation of the cluster operator, then this is the largest uncertainty so far.

Finally, we quantify the uncertainty due to the omission of the SRG-induced four- and more-nucleon interactions through the α dependence of the CCSD and Λ-CCSD(T) results shown in Fig. 4 and Tables I and II. First of all, we note that missing many-body terms of the Hamiltonian are of opposite sign but of the same order of magnitude for the $NN + 3N$–induced and the $NN + 3N$–full Hamiltonian. For the $NN + 3N$–induced Hamiltonian the ground-state energies for $\alpha = 0.02\,\mathrm{fm}^4$ (harder interaction) are systematically lower than for $\alpha = 0.08\,\mathrm{fm}^4$ (softer interaction). Furthermore, the energy spread over this range of flow parameters is smaller for CCSD and larger for Λ-CCSD(T). For ^{40}Ca, e.g., the spread amounts to 3% of the ground-state energy in CCSD and 5% in Λ-CCSD(T). The pattern is reversed for the $NN + 3N$–full Hamiltonian. The ground-state energies for $\alpha = 0.02\,\mathrm{fm}^4$ are systematically above the energies for $\alpha = 0.08\,\mathrm{fm}^4$ and the energy spread is reduced by including the triple correction. For ^{40}Ca the relative energy spreads are 5% for the CCSD and 2% for Λ-CCSD(T). Note that these α dependencies are distorted by the influence of the $E_{3\,\max}$ truncation. With increasing $E_{3\,\max}$ the Λ-CCSD(T) ground-state energies will move up for harder interactions and, thus, the apparent α dependence will be reduced for $NN + 3N$ induced and increased for $NN + 3N$ full.

If we compare the ground-state energies throughout the set of nuclei discussed here with the experiment (cf. Fig. 4), keeping in mind the uncertainties we discussed above, then the agreement is remarkable. We stress that no information beyond $A = 4$ was used to constrain the Hamiltonian, so obtaining the correct binding systematics for medium-mass nuclei is far from trivial. Though the impact of the initial chiral $3N$ interaction is moderate on the scales shown in Fig. 4, it is important to obtain the correction binding-energy systematics along isotopic chains. In contrast, the effect of the SRG-induced

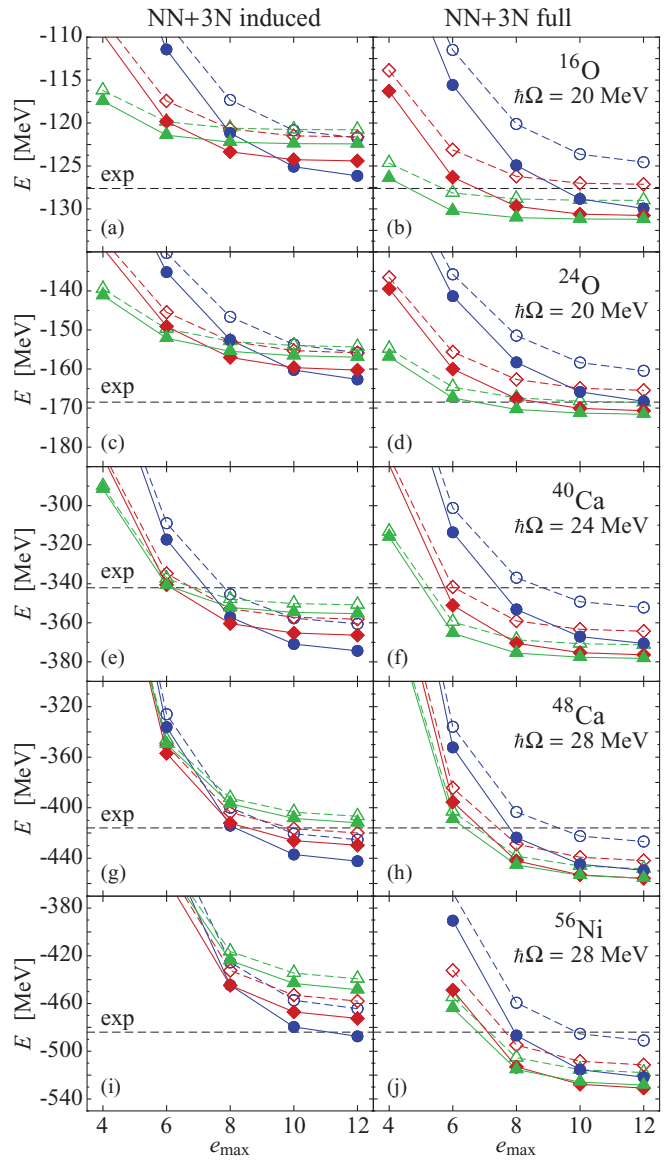

FIG. 4. (Color online) Λ-CCSD(T) (solid lines) and CCSD (dashed lines) ground-state energies for ^{16,24}O, ^{40,48}Ca, and ^{56}Ni as function of $e_{\max}$ for the two types of Hamiltonians (see column headings) using the NO2B approximation for flow parameters: $\alpha = 0.02\,\mathrm{fm}^4$ (●), $0.04\,\mathrm{fm}^4$ (◆), and $0.08\,\mathrm{fm}^4$ (▲).

$3N$ interactions is huge and their inclusion is mandatory—for ^{56}Ni and $\alpha = 0.08\,\mathrm{fm}^4$ a calculation with only SRG-evolved NN interactions yields an unphysical ground-state energy of about -950 MeV.

Conclusions. We have presented the first *ab initio* calculations for nuclei in the medium-mass regime with inclusion of explicit $3N$ interactions. On this baseline we quantify the effects of all truncations in the many-body approach, i.e., the cluster rank of the CC ansatz, the single-particle truncation $e_{\max}$, the truncation of the $3N$ matrix elements $E_{3\,\max}$, and the optional omission of residual normal-ordered $3N$ terms. For all truncations we clearly benefit from the prediagonalization of the Hamiltonian through the SRG evolution—for Hamiltonians with $\alpha = 0.08\,\mathrm{fm}^4$ the uncertainties due to the

$E_{3\,\mathrm{max}}$ truncation and the NO2B approximation are at the level of 1% or below and the effect of the triple correction is only 2%. In particular the impacts of the $E_{3\,\mathrm{max}}$ truncation and the triple corrections increase rapidly when going to harder interactions. The omission of SRG-induced four- and many-body terms, i.e., the truncation of the particle rank of the Hamiltonian, introduces an uncertainty at the level of a few percent and thus limits the overall accuracy of the approach. Reduction or elimination of this uncertainty will be a prime goal of future studies. Finally, our results point towards the predictive power of chiral $NN + 3N$ Hamiltonians for medium-mass nuclei.

Acknowledgments. Numerical calculations have been performed at the Jülich Supercomputing Centre, the LOEWE-CSC Frankfurt, and the National Energy Research Scientific Computing Center and were supported by the Office of Science of the US Department of Energy under Contract No. DE-AC02-05CH11231, the Deutsche Forschungsgemeinschaft through Contract SFB 634, the Helmholtz International Center for FAIR within the LOEWE program of the State of Hesse, and the BMBF through Contracts No. 06DA9040I and No. 06DA7047I. P.N. acknowledges support from Natural Sciences and Engineering Research Council of Canada (NSERC) through Grant No. 401945-2011.

[1] M. Włoch, D. Dean, J. R. Gour, M. Hjorth-Jensen, K. Kowalski, T. Papenbrock, and P. Piecuch, Phys. Rev. Lett. **94**, 212501 (2005).
[2] G. Hagen, T. Papenbrock, D. J. Dean, and M. Hjorth-Jensen, Phys. Rev. Lett. **101**, 092502 (2008).
[3] G. Hagen, M. Hjorth-Jensen, G. R. Jansen, R. Machleidt, and T. Papenbrock, Phys. Rev. Lett. **109**, 032502 (2012).
[4] V. Somá, T. Duguet, and C. Barbieri, Phys. Rev. C **84**, 064317 (2011).
[5] K. Tsukiyama, S. K. Bogner, and A. Schwenk, Phys. Rev. Lett. **106**, 222502 (2011).
[6] H. Hergert, S. K. Bogner, S. Binder, A. Calci, J. Langhammer, A. Schwenk, and R. Roth, arXiv:1212.1190v1 [nucl-th].
[7] P. Navrátil, S. Quaglioni, I. Stetcu, and B. Barrett, J. Phys. G: Nucl. Part. Phys. **36**, 083101 (2009).
[8] R. Roth, Phys. Rev. C **79**, 064324 (2009).
[9] R. Roth and P. Navrátil, Phys. Rev. Lett. **99**, 092501 (2007).
[10] R. Machleidt and D. R. Entem, Phys. Rep. **503**, 1 (2011).
[11] E. Epelbaum, H.-W. Hammer, and U.-G. Meißner, Rev. Mod. Phys. **81**, 1773 (2009).
[12] D. R. Entem and R. Machleidt, Phys. Rev. C **68**, 041001(R) (2003).
[13] E. Epelbaum, W. Glöckle, and U.-G. Meißner, Nucl. Phys. A **747**, 362 (2005).
[14] P. Navrátil, Few Body Syst. **41**, 117 (2007).
[15] P. Navrátil, V. G. Gueorguiev, J. P. Vary, W. E. Ormand, and A. Nogga, Phys. Rev. Lett. **99**, 042501 (2007).
[16] P. Maris, J. P. Vary, P. Navrátil, W. E. Ormand, H. Nam, and D. J. Dean, Phys. Rev. Lett. **106**, 202502 (2011).
[17] P. Maris, J. P. Vary, and P. Navrátil, Phys. Rev. C **87**, 014327 (2013).
[18] R. Roth, J. Langhammer, A. Calci, S. Binder, and P. Navrátil, Phys. Rev. Lett. **107**, 072501 (2011).
[19] V. Bernard, E. Epelbaum, H. Krebs, and U.-G. Meißner, Phys. Rev. C **77**, 064004 (2008).
[20] V. Bernard, E. Epelbaum, H. Krebs, and U.-G. Meißner, Phys. Rev. C **84**, 054001 (2011).
[21] R. Skibiński, J. Golak, K. Topolnicki, H. Witala, E. Epelbaum, W. Glöckle, H. Krebs, A. Nogga, and H. Kamada, Phys. Rev. C **84**, 054005 (2011).
[22] H. Krebs, E. Epelbaum, and U.-G. Meißner, Eur. Phys. J. A **32**, 127 (2007).
[23] G. Hagen, M. Hjorth-Jensen, G. R. Jansen, R. Machleidt, and T. Papenbrock, Phys. Rev. Lett. **108**, 242501 (2012).
[24] R. Roth, S. Binder, K. Vobig, A. Calci, J. Langhammer, and P. Navrátil, Phys. Rev. Lett. **109**, 052501 (2012).
[25] E. D. Jurgenson, P. Navrátil, and R. J. Furnstahl, Phys. Rev. Lett. **103**, 082501 (2009).
[26] G. Hagen, T. Papenbrock, D. J. Dean, A. Schwenk, A. Nogga, M. Włoch, and P. Piecuch, Phys. Rev. C **76**, 034302 (2007).
[27] I. Shavitt and R. Bartlett, *Many-Body Methods in Chemistry and Physics* (Cambridge University Press, Cambridge, 2009).
[28] G. Hagen, T. Papenbrock, D. J. Dean, and M. Hjorth-Jensen, Phys. Rev. C **82**, 034330 (2010).
[29] R. Roth, A. Calci, J. Langhammer, and S. Binder (unpublished).
[30] A. G. Taube and R. J. Bartlett, J. Chem. Phys. **128**, 044110 (2008).
[31] A. G. Taube and R. J. Bartlett, J. Chem. Phys. **128**, 044111 (2008).